Supporting Information of

Broadband Quantum Efficiency Enhancement in High Index Nanowires Resonators

Yiming Yang,[1] *Xingyue Peng,*[1] *Steven Hyatt,*[1] *and Dong Yu*[1*]

[1]Department of Physics, University of California, Davis, CA 95616, USA

1. Comparison of Refractive Indices of Various Materials

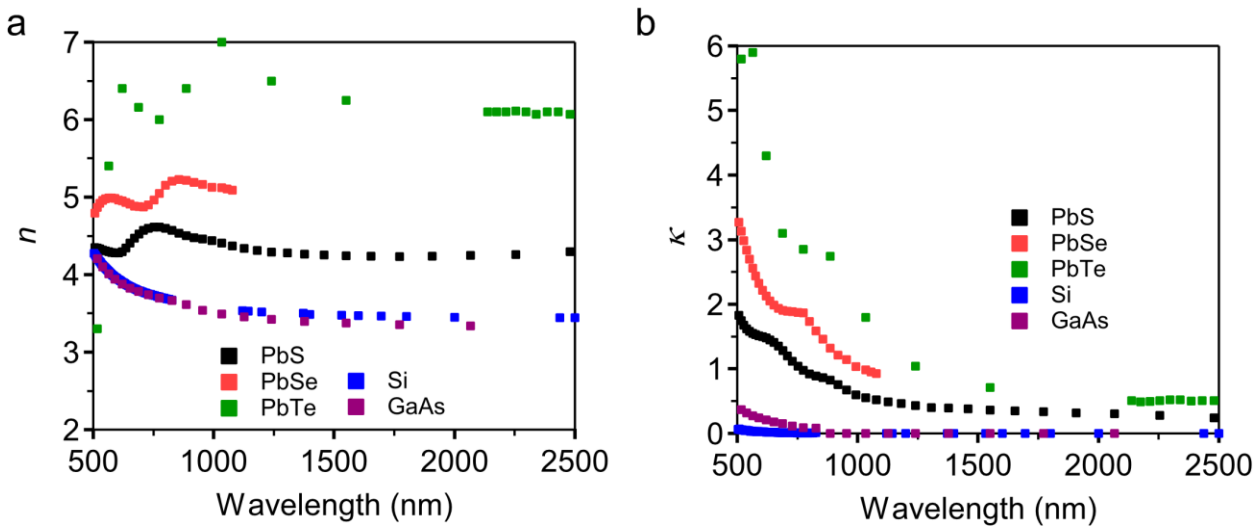

Figure S1. (a)&(b) The real (n) and imaginary (κ) parts of the complex indices of refraction of PbS, PbSe, PbTe, Si and GaAs in the visible and near infrared spectrum. The n & κ data is acquired from *Handbook of Optical Constants of Solids, Edward D. Palik, Academic Press, 1998.* In FDTD simulations of PbS NWs, n & κ as a function of wavelength are fitted by polynomial functions, with standard deviation below 0.1.

2. Details of EQE Calculation and Error Analysis

EQE is defined as the ratio of the number of electrons collected to the number of incident photons projected to the physical area of the NW, that is,

$$EQE = \frac{I_{sc} \cdot h\nu}{q \cdot P_{NW}} \tag{1}$$

where I_{sc} is the short-circuit current, P_{NW} is the power of laser beam projected onto the physical area of the NW (Figure S2(a)).

In our experiments, we use a focused laser beam whose intensity profile satisfies the Airy diffraction pattern, which can be approximated by a Gaussian distribution,

$$Int = I_0 \cdot e^{\frac{-(x^2+y^2)}{|W_{laser}|^2}} \tag{2}$$

where I_0 is determined by measuring the total power of the laser P_{tot},

$$P_{tot} = \iint Int\, dxdy = \pi \cdot |W_{laser}|^2 \cdot I_0 \tag{3}$$

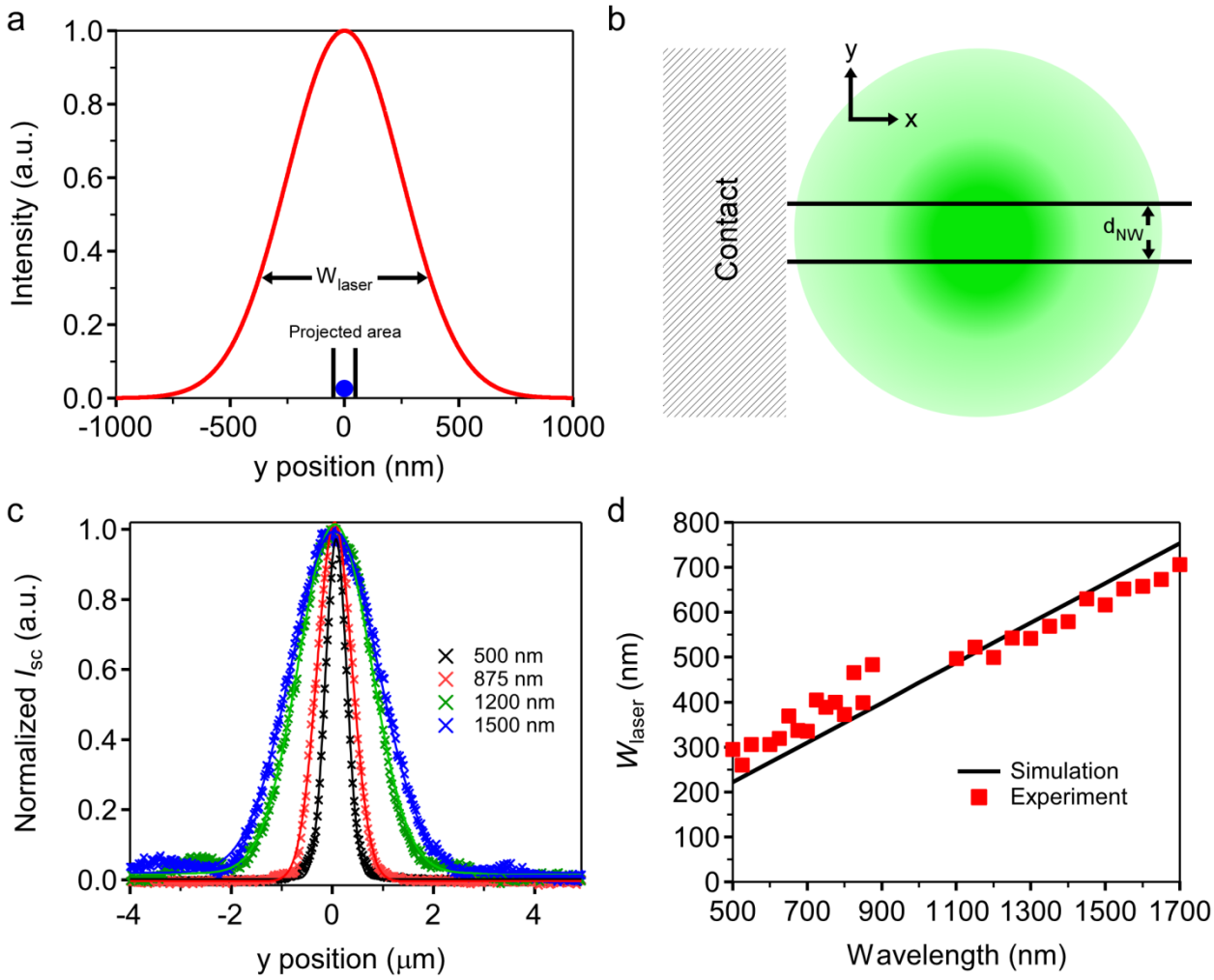

Figure S2. (a) Gaussian profile of the focused laser intensity. The peak is centered at x = 0 nm, with W_{laser} = 354 nm. The NW is also centered at x = 0 nm, with d_{NW} = 60 nm. (b) Schematic diagram of laser spot focused near the contact. Note that the graph is not scaled to the actual size. (c) Photocurrent cross sections perpendicular to the NW axis (along y-axis) extracted from SPCM at representative wavelengths. The solid lines are the Gaussian fittings where W_{laser} can be extracted. The W_{laser} is defined as $\sqrt{2}$ times standard deviation of the Gaussian fit. (d) Wavelength-dependent W_{laser}. The solid line is the simulated width from FDTD simulation, with NA = 0.97 and filled lens condition, which is in excellent agreement with the experimental observation.

When the distance between the injection and the contact is much longer than W_{laser} (which is truly the experimental situation for the peak photocurrent since the PbS NWs have minority diffusion lengths much longer than W_{laser}), P_{NW} can be approximately calculated by integrating over the entire x axis (Figure S2(b)),

$$P_{NW} = \int_{-\infty}^{\infty} dx \int_{-d/2}^{d/2} dy \; I_0 \cdot e^{\frac{-(x^2+y^2)}{|W_{laser}|^2}}$$

$$= \sqrt{\pi} I_0 \cdot W_{laser} \cdot \int_{-d_{NW}/2}^{d_{NW}/2} e^{\frac{-y^2}{|W_{laser}|^2}} dy \quad (4)$$

As shown in Figure S2 (a), $W_{laser} >> d_{NW}$ and equation (4) can be simplified to,

$$P_{NW} = \sqrt{\pi} I_0 \cdot W_{laser} \cdot d_{NW} \quad (5)$$

Insert equations (5) and (3) to equation (1), the EQE can then be expressed as,

$$EQE = \frac{\sqrt{\pi} \cdot I_{sc} \cdot h\nu \cdot W_{laser}}{q \cdot P_{tot} \cdot d_{NW}} \quad (6)$$

Experimentally, I_{sc} was measured through a current preamplifier (DL Instruments, model 1211) and a National Instrument (NI) data acquisition system. W_{laser} was obtained by fitting the cross section perpendicular to the NW in the SPCM image (Figure S1(c)). P_{tot} was directly measured with a power meter (THORLABS, model PM100) under the objective lens. d_{NW} was measured with an atomic force microscope (VEECO Dimension 3100).

The errors for I_{sc}, W_{laser}, P_{tot}, and d_{NW} are estimated below,

$$\frac{\Delta_{I_{sc}}}{I_{sc}} < 0.1\% ;$$

$$\frac{\Delta_{W_{laser}}}{W_{laser}} = 0.5\%;$$

$$\frac{\Delta_{d_{NW}}}{d_{NW}} = 5\% ;$$

$$\frac{\Delta_{P_{tot}}}{P_{tot}} = 5\% \text{ (visible), } 20\% \text{ (infrared);}$$

Note that the 20% error of infrared P_{tot} is due to the power fluctuation of the Ge sensor (THORLABs, model s122b). The error of d_{NW} originated from the amorphous surface oxide layer outside the NW, which typically has a thickness of 1 to 5 nm.

The overall error of EQE is:

$$\frac{\Delta_{EQE}}{EQE} = \sqrt{(\frac{\Delta_{I_{sc}}}{I_{sc}})^2 + (\frac{\Delta_{W_{laser}}}{W_{laser}})^2 + (\frac{\Delta_{d_{NW}}}{d_{NW}})^2 + (\frac{\Delta_{P_{tot}}}{P_{tot}})^2} \quad (7)$$

$$= 8.7\% \text{ (visible), } 21.2\% \text{ (infrared)}$$

Another concern is that the finite diameter of NW may cause overestimation of W_{laser} when extracting W_{laser} from fitting the perpendicular photocurrent cross section (Figure S2(c)). However, careful quantitative analysis shows that the overestimation in W_{laser} caused by a finite d_{NW} is insignificant for NWs with diameter smaller than 100 nm and hence can be ignored. We have also simulated the intensity distribution at the focal plane using FDTD simulation (solid line in Figure S2(d)). The experimentally determined W_{laser} agrees very well with the simulation results. In the infrared range, the experimental value is slightly smaller than the simulated value, which may be due to the change of objective lens NA (0.97) for longer wavelength. We calculate EQE based on the experimental values of W_{laser}.

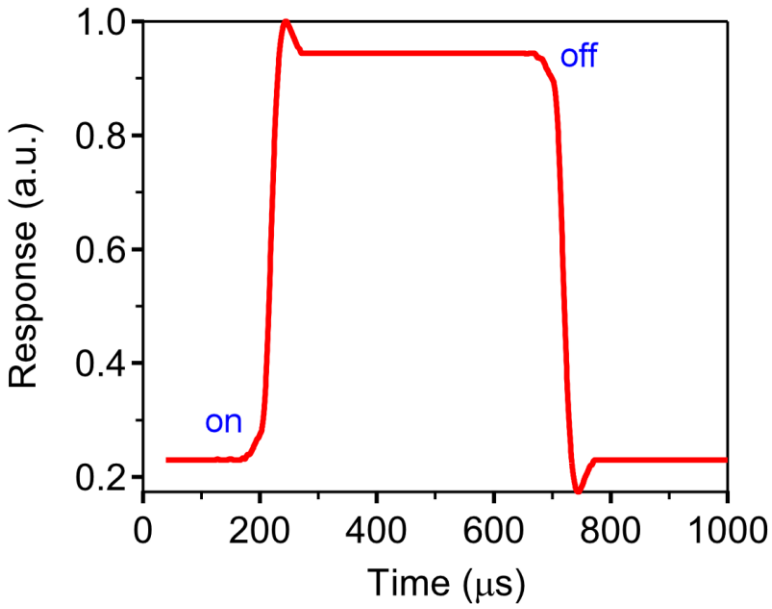

Figure S3. Temporal photoresponse of a PbS NW Schottky device at V_{sd} = 0 V. The laser focused on near the Schottky contact is modulated by an optical chopper rotating at 1000 Hz and the photocurrent is modulated with a preamp and a digital oscilloscope.

In addition, we measured the photo-response time of the NW devices (Figure S3). Our devices have fast photo-response with rise/fall time shorter than 25 μs. The actual response time can be even faster as the measurement is limited by the temporal resolution of our pre-amplifier. The fast response time allows a rapid acquisition of SPCM images. Each 400x400 image takes less than 2 minutes. We have confirmed that photocurrent is independent of scanning rates.

3. Details of FDTD Simulation

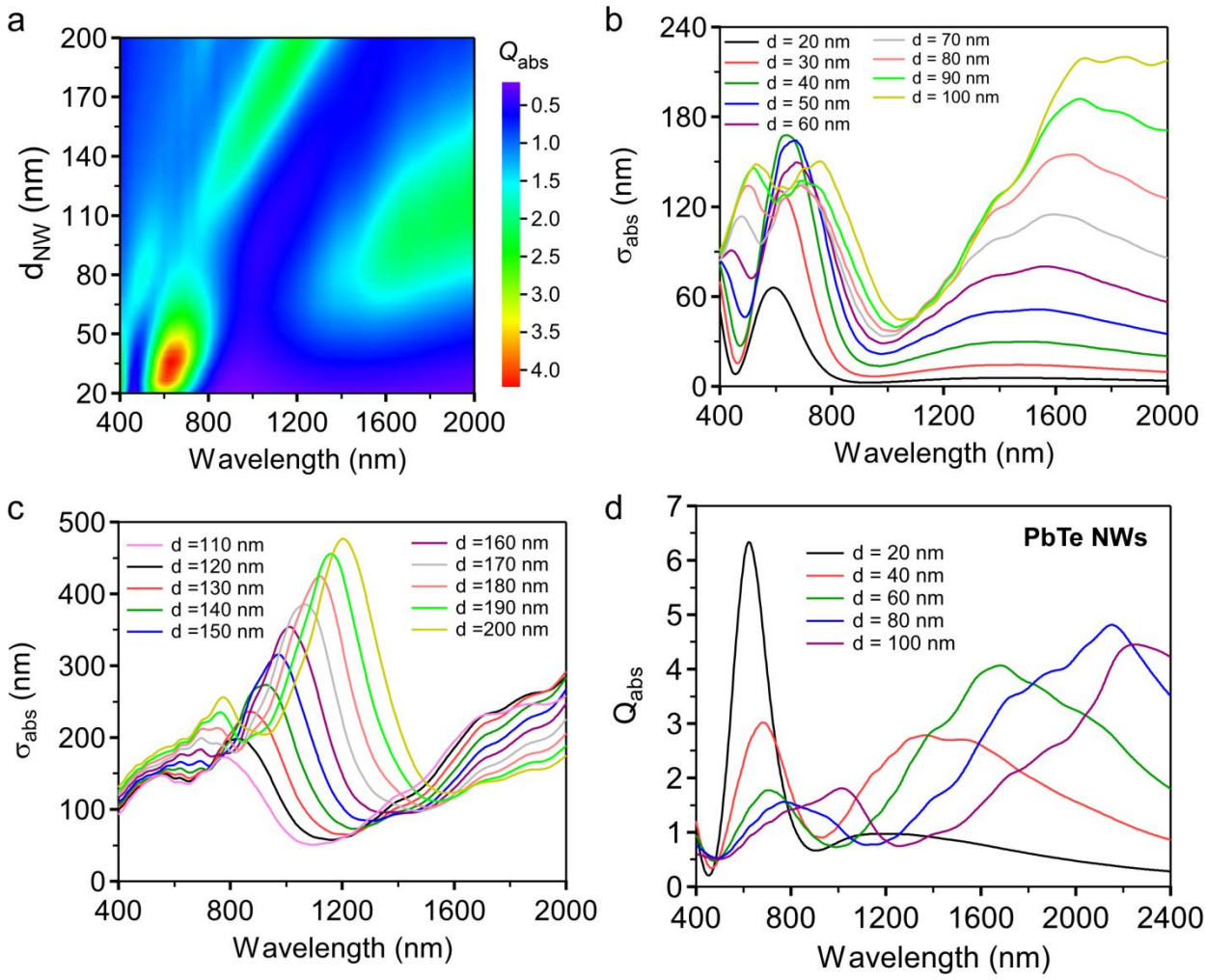

Figure S4. (a) 2D plot of Q_{abs} as a function of the NW diameter and wavelength. Same as the plot shown in the main text but plotted in a different way here. (b)&(c) σ_{abs} plotted as a function of wavelength for various NW diameters. Note that the plots show clearly a shift of the resonance peaks with the wavelength and the possibility of broadband capture of sunlight by using diameter-varying (tapered) NWs. (d) Wavelength-dependent Q_{abs} for PbTe NWs with different diameters. Note Q_{abs} can reach 6 in PbTe because of its larger n and κ values. In comparison, maximum Q_{abs} in PbSe is 4.47 as shown in (a).

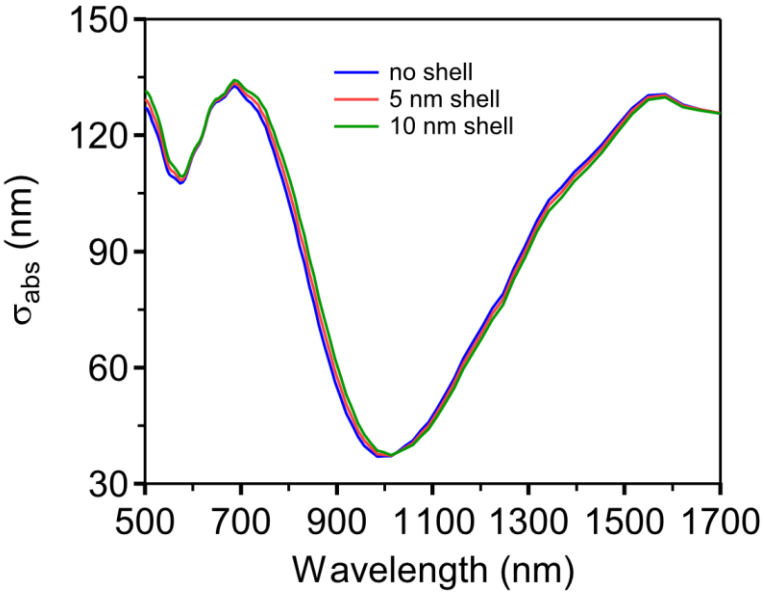

Figure S5. Comparison of FDTD simulated absorption spectra among NWs with no shell, 5 nm SiO_2 shell, and 10 nm SiO_2 shell, showing the shell thickness does not have much influence. The PbS NWs have been shown to have a thin coating of SiO_2. The diameter of the PbS NW core is 70 nm.

4. *I*-V_{sd} Curves In the Dark and Under Illumination

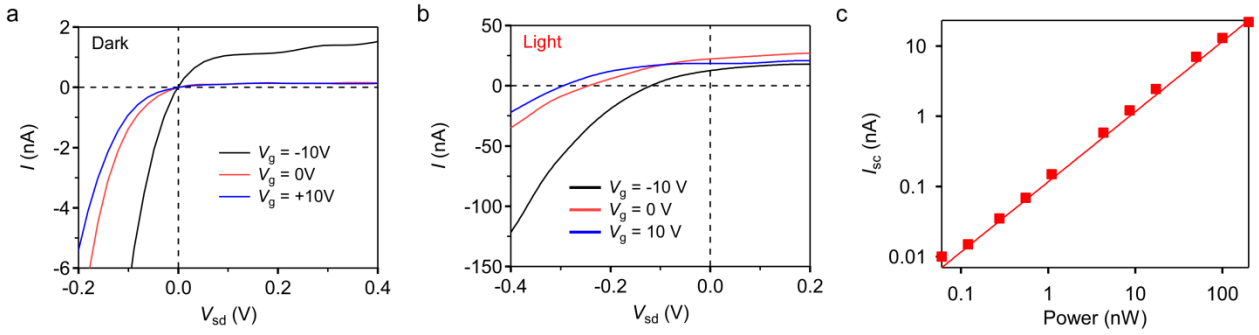

Figure S6. (a)&(b) Dark/light *I*-V_{sd} curves at V_g = 0, +10V, and -10V. A clear increase of dark saturation current can be observed at negative V_g which correlates with a decrease of V_{oc} shown in (b). This observation strongly supports the mechanism proposed in the main text that the negative V_g leads to increased leakage current through the Schottky junction. (c) I_{sc} plotted as a function of laser power. A linear intensity dependent photocurrent is observed over 3 orders of magnitude, indicating nonlinear effects such as high carrier injection induced band profile change can be ignored in this study.

5. Gate Dependent Photocurrent Decay Length

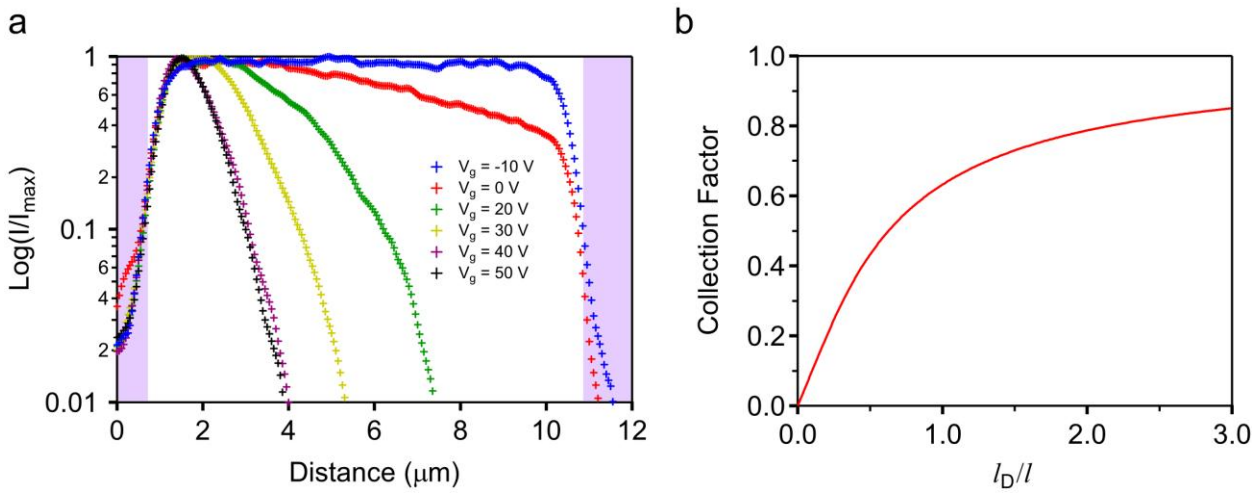

Figure S7. (a) Gate-dependent photocurrent as a function of injection position. The shaded areas represent the two contacts. (b) Collection factor as a function of l_D/l.

The collection factor is defined as:

$$Collection\ Factor = \frac{charge\ collected}{charge\ injected} = \frac{\int_0^l e^{-\frac{x}{l_D}} dx}{l} = \frac{l_D}{l}\left(1 - e^{-\frac{l}{l_D}}\right) \quad (8)$$

where l_D is the minority diffusion length, l is the device channel length.

6. Polarization Dependence of Photocurrent

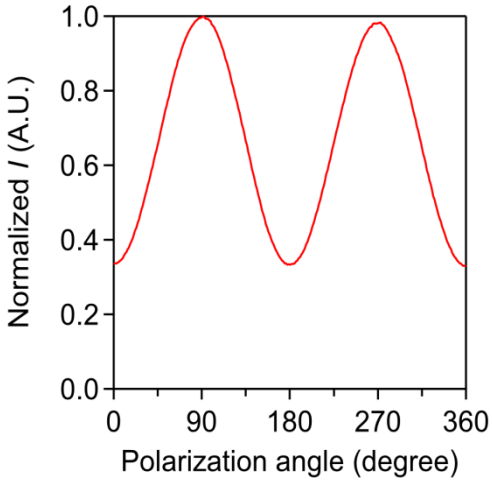

Figure S8. Photocurrent as a function of polarization angle. Zero degree refers to polarization angle perpendicular to the nanowire axis.

In the FDTD simulation, we used transverse-magnetic (TM) mode where the light polarization direction is along the nanowire axis. Under this configuration, the light absorption is generally much stronger compared to the transverse-electric (TE) mode, as demonstrated experimentally in Figure S8. Therfore, we focus on the parallel polarization case in this work.